Effects of serpentinization degree on the geotechnical characteristics of ultramafic rocks in the southwest of Mashhad city (Iran)

Salameh Afshar[1], Mohammad Ghafoori[2]*, Naser Hafezi Moghadas[2], Gholam Reza Lashkaripour[2]
[1] *Faculty of Science, Ferdowsi University of Mashhad, International Campus, Mashhad, Iran*
[2] *Department of Geology, Faculty of Science, Ferdowsi University of Mashhad, Iran*
**Corresponding author, e–mail: e-mail: Ghafoori@um.ac.ir*
(*received: 07/11/2018 ; accepted: 27/01/2019*)

Abstract
The present work was conducted to investigate the geotechnical properties of two meta-peridotites and meta-pyroxenites of an ultramafic complex mainly consisting of ultramafic rocks. For this purpose, microscopic studies were performed to determine the percentage of serpentinization in these rocks. In addition, a number of mechanical and physical tests were performed on collected samples with different serpentinization grades to determine their geotechnical properties. Finally, the serpentinization degree and geotechnical results were compared for meta-peridotites and meta-pyroxenites. The results revealed a closed relationship among the serpentinization degree, Brazilian tensile strength (BTS), uniaxial compressive strength (UCS), and density. Due to the high costs of the UCS test, this study attempts to establish a relationship between these parameters. To demonstrate the relationship between these parameters, the obtained results are presented as a single graph. So, the UCS can be estimated based on the BTS, density, and the serpentinization degree. The results showed that the field behavior of rock masses also could be used to predict the UCS) range and degree of serpentinization. Overall, these results can be useful for determining the geotechnical properties of these rocks.

Keywords: *Ultramafic Rocks, Serpentinization Degree, Geotechnical Properties.*

Introduction

Ophiolitic associations in folded belts represent fragments of ancient oceanic crust. These rocks are retained in suture zones (Promyslova *et al.*, 2016), which form by spreading of only one tectonic setting; i.e., the mid-ocean ridges (Khanchuk & Vysotskiy, 2015). Dobretsov was among the first who reported different types of ophiolites and correspondingly, different settings of their formation (Dobretsov, 1974; Dobretsov *et al.*, 1994). For classification of ophiolites, this author used both structural features of rocks and data on their metamorphism and geochemistry. In this regard, Miyashiro (1975) holds a similar viewpoint. However, there is no consensus among researchers on the number the type of ophiolites (Coleman, 1977; Hynes, 1975; Moores, 1975). Some of them have reported two to three (Dobretsov, 1980; Dobretsov *et al.*, 1977, 1986; Markov *et al.*, 1977; Shcheglov *et al.*, 1984; Vysotskiy, 1989, 1996) while some others have reported six to seven (Dobretsov, 1985) types of ophiolites. The recognized types of ophiolites had the characteristics of the tectonic settings they formed in; e.g., oceanic plates, island-arc systems, and transform faults (Khanchuk & Vysotskiy, 2015). Ophiolitic rocks exhibit a wide range of chemical compositions and petrographic features; hence, the existence of lithotypes with substantially different engineering properties is very common even in the same suite. Fresh ophiolitic rocks have exceptional engineering characteristics. The effect of ocean-floor metamorphism variously changes their physicomechanical properties (Rigopoulos, 2009; Rigopoulos *et al.*, 2010, 2012, 2013). The impact of alteration on the strength parameters of rocks has attracted the attention of many scientists such that various chemical and microphotographic indices have been proposed. Most studies have focused on granitic rocks (e.g. Arel and Tuğrul, 2001; Přikryl, 2006; Ceryan *et al.*, 2008). A significant number of studies have also investigated the influence of hydrothermal alteration on the physical and mechanical properties of volcanic rocks (Pola *et al.*, 2012, 2014; Siratovich *et al.*, 2014; Wyering *et al.*, 2014). Rigopoulos *et al.* (2010) proposed micropetrographic indices for the engineering assessment of mafic ophiolitic rocks. There are also a few studies that have been concentrated on the modification of the mechanical behavior of ultramafic ophiolitic rocks due to changes in their petrographic characteristics and chemical composition during hydrothermal alteration (Kiliç *et al.*, 1998; Rigopoulos *et al.*, 2012; Ündül & Tuğrul, 2012). This focus of this research is on ultrabasic rocks, which cover a wide range of rock types (e.g., harzburgites, lherzolites, plagioclastic peridotites, and dunites). Due to ocean-floor metamorphism (serpentinization), the petrographic characteristics of these rocks are severely changed. Variations in mineralogical and textural characteristics as well as the serpentinization affect their physicomechanical properties, which vary from excellent to fair, becoming poor to very poor when extensive alteration and/or intense information exists (Christensen 1966, 2004; Ramana *et al.*, 1986; Escartin *et al.*, 2001; Marinos *et al.*, 2006; Diamantis, 2010; Ozsoy *et al.*, 2010). The most commonly used and fundamental mechanical parameter is the uniaxial compressive strength (UCS), which is directly determined according to International Society for Rock Mechanics (ISRM, 2007). Despite its relative simplicity, this method is time-consuming, expensive, and requires a large number of well-prepared (regularly shaped) rock specimens. Weak, highly fractured, thinly bedded, block-in-matrix, and highly to completely serpentinized ultrabasic rocks and sheared serpentinites are usually not suitable for preparing specimens. Thus, determination of the UCS is usually difficult for these types of rocks. For this reason, UCS has been largely replaced by indirect, simpler, faster, and more economical tests (Sonmez *et al.*, 2004, 2006). Although many attempts have also been made to correlate the UCS with certain physical and mechanical characteristics, only few studies have been concentrated on serpentinites (Rao & Ramana, 1974; Koumantakis, 1982; Paventi *et al.*, 1996; Christensen, 2004; Courtier *et al.*, 2004; Marinos *et al.*, 2006). This study presents the serpentinization degree and the physical and mechanical parameters. Moreover, it offers some empirical equations between UCS and the above-mentioned parameters through the simple, fast, practical, and economical estimation of UCS in ultramafics. Within the framework of the present study, a total of 313 samples were collected from the southwest of Mashhad city in the northeast of Iran (Fig. 1) and their thin sections were studied. After the lithology separating and determining the serpentinization degree in lithological units, 60 samples including 30 meta-peridotites and 30 meta-pyroxenites with different percentages of serpentine were selected and rock blocks were provided for coring. Then, the samples were tested to determine physical and mechanical characteristics. The results were statistically analyzed, the relationships among these parameters were described by the best-fit equations, and the highest coefficient of determination in each relationship was also determined. Finally, based on the results obtained and considering the degree of serpentinization, a graph was proposed to predict the resistance. Next, laboratory results were compared with field observations and interpreted.

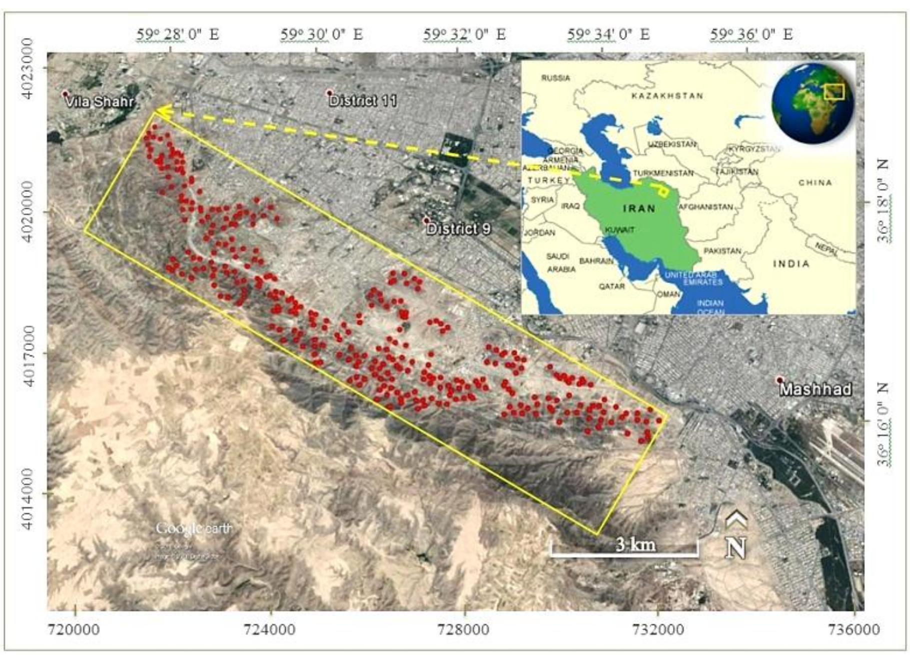

Figure 1. Location of samples taken from the study area (southwest of Mashhad).

Geological setting

In the early Paleozoic, a rift formed and expanded between Iran and Turan plates that led to the conversion of the continent to sea and sea to the ocean, and eventually the formation of the Paleo-Tethys Ocean. Finally, in the late Paleozoic, the ocean was gradually closed and its subduction toward North resulted in some changes in the north of Iran. One of these changes is the regional metamorphism of ophiolite complex together with the sedimentary rocks in the greenschist facies and formation of serpentines in the area. In this regard, serpentine is typical of ophiolites that can form by alteration, weathering, and regional metamorphism (Faust & Fahey, 1964).

The serpentine resulting from ophiolite alteration has limited zone and chromite mineralization occurs in them. In the study area, the serpentines widely spread so that they have been reported from Europe to the northeast of Iran and Afghanistan ((Boulin, 1988; Stampfli, 1996; Zanchi *et al.*, 2009; Abdelaziz *et al.*, 2018).

The serpentine resulting from ophiolite weathering forms nickel laterites. Although the study area has arid and semi-arid climate and serpentines can be seen in trenches up to 30 m depth, no nickel is observed in these rocks. Therefore, it can be inferred that the serpentines of the study area did not form through weathering.

In serpentines formed by regional metamorphism of ophiolites and in sediments of ophiolites, the clays of shale and marl altered to micas. Then, micas form slate stone by placing perpendicular to the pressure. Accordingly, slates in the study area, together with serpentines (Fig. 2), show a low-grade regional metamorphism.

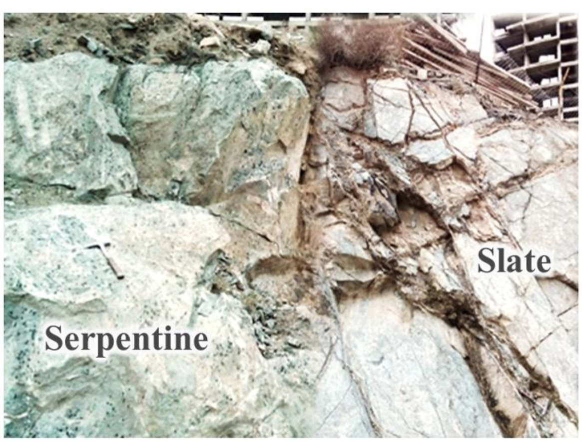

Figure 2. Slates together with serpentines in the study area

After subduction of oceanic crust and regional metamorphism of ophiolite, the Paleo-Tethys Ocean was completely closed in the middle Triassic and the ophiolites were thrusted. The tectonics of the region has been active since middle Triassic due to the presence of main thrust faults. Therefore, the serpentines formed by metamorphism show different degrees of thrusts-induced serpentinization.

Methods

To conduct the lithological studies, 313 samples were collected from natural outcrops and trenches existing in the studied area. Following the preparation of the microscopic thin section, the mineralogical characteristics, texture changes, color changes, degradation, and microcrack development were studied. Then, the samples were classified based on the general classification of ultramafic rocks (Streckeisen, 1974). In this classification, the ultramafics extracted from the studied area were grouped in the meta-peridotite and meta-pyroxenite rocks. After the lithology separating and determining the percentage of serpentinization in lithological units, 60 samples with the different percentages of serpentine were selected and rock blocks were provided for coring. Then, the mechanical tests including UCS, point load strength (Is50), and Brazilian tensile strength (BTS) were carried out in the laboratory of Ferdowsi University of Mashhad. Also, the physical test (i.e., density, water absorption, and porosity) were performed in this laboratory. Regression analysis was performed on the serpentinization degree and engineering parameters of the studied ultramafic rocks. Moreover, a few correlations among selected engineering parameters were calculated. Since, according to the results, the degree of serpentinization affects the resistance of the studied rocks, it should be considered in the relationship between the parameters proposed. Accordingly, the mechanical and physical parameters that had the closest relationship were determined. Moreover, considering the degree of serpentinization, a graph was prepared for them in order to predict the parameters presented in the graph more precisely than the equations. Finally, the results were compared with field observations and presented in a table.

Results

Petrographic analysis

The Mashhad ultramafics mainly consist of meta-peridotites and meta-pyroxenites with different percentage of serpentinization because of tectonic events. To conduct the lithological studies, 313 macroscopic samples of the natural outcrops and trenches existing in the study area were collected. For this purpose, we used an automatic counter mounted on a Leitner microscope to determine the secondary elements formed in the samples accurately. The mineralogy of both groups is described in the following.

Meta peridotites:
Meta-dunites with more than 90% Olivine are the main meta-peridotites of the region. These rocks are generally intact and have a granular texture. In all segments, with an increased percentage of serpentinization, it is clearly seen that the serpentines are replaced with Olivine. Consequently, in these specimens, the mesh texture along with the granular texture is observed as a result of an increased percentage of serpentinization. Other major meta-peridotites in this area are meta-Harzburgites, meta-Lherzolite, and meta-Wehrlite in which Orthopyroxenes and Clinopyroxene existed together with Olivine. In these rocks, Olivine is converted into Serpentine with an increase in the percentage of serpentinization; however, a greater fracturing is observed in orthopyroxenes (Fig. 3A).

Meta-pyroxenites:
The other ultramafic group of the region is meta-pyroxenites. In meta-pyroxenites, the amount of Pyroxene mineral is increased over 60% while the amount of olivine mineral is reduced to less than 40%. The texture of this group of rocks is also granular. With increased serpentinization, a subsequent increase in the number of fractures and fine cracks is observed in these rocks. The formation of mineralized Tremolite is seen with the increased serpentinization in meta-pyroxenites containing Orthopyroxenes (Fig. 3B) and deposits of Talc, and in the meta-pyroxenites containing clinopyroxene (Fig 3C).

These two groups of ultramafic rocks in the study area, due to the pressure and temperature, have undergone regional metamorphisms that have ultimately led to the formation of serpentines. Subsequently, tectonic creates different percentages of serpentinization in the region. The primary rock events are not readily recognizable at high levels of serpentinization. These rocks appear in pistachio green and light or dark green and are brighter than other fragments. In the thin sections, they generally have a mesh texture while in completely serpentinization levels, strand textures are seen. As shown in Fig. 3D, because of the serpentinization process, only circular casts of olivine remain, which are filled by serpentine.

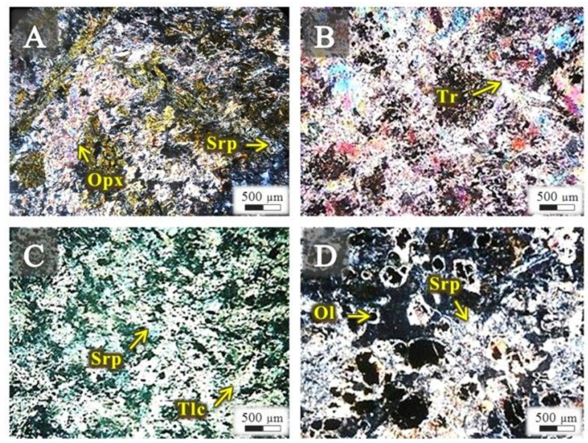

Figure 3. A. Increased fracture and microfracture in orthopyroxene (Opx) with increased serpentinization; B. Conversion of Clinopyroxene to Thermolite (Tr); C. Conversion of Orthopyroxene to Talc (Tlc); and D. Maintaining Olivine circular molds by increasing serpentinization

Mechanical properties
In this study, to compare the samples in terms of mechanical properties and their serpentinization percentage, samples that were very similar in the thin section were removed and finally 60 samples including 30 samples of meta-peridotite and 30 samples of meta-pyroxenite underwent geotechnical characterizations. Then, to determine the mechanical properties of ultramafic rocks, UCS, Point load (Is50), and BTS tests were performed on core samples. Is50 test was performed on blocky or core samples (axial test) according to ISRM (1985). BTS tests and UCS tests were carried out according to the methods proposed by ISRM (1978) and ISRM (1979), respectively.

Among the geotechnical parameters, UCS is one of the most utilized mechanical parameters of rock that is used in designs more than other parameters (Bieniawski, 1974). Due to the importance of this parameter in engineering projects, the samples were classified according to the standard UCS (ISRM, 1979) presented in Table 1. According to this classification, Meta-peridotites and Meta-pyroxenites of the region are classified into three classes of Medium Strong (MS), Strong (S), and Very Strong strength (VS).

Table 2 presents the results of mechanical tests and the serpentinization percentage in meta-peridotites and meta-pyroxenites.

Table 1. Classification of rocks (ISRM, 1979) based on UCS

Classification	uniaxial compressive strength (UCS) (MPa)
Very Weak (VW)	1 - 5
Weak (W)	5 - 25
Medium Strong (MS)	25 - 50
Strong (S)	50 - 100
Very Strong (VS)	100 - 250
Extra Strong (ES)	> 250

Table 2. Results of mechanical experiments performed on meta-peridotites and meta-pyroxenites

Meta peridotites						Meta pyroxenites					
Resistive classification	Sample number	UCS (MPa)	Is 50 (MPa)	BTS (MPa)	Serpentinization (%)	**Resistive classification**	Sample number	UCS (MPa)	Is 50 (MPa)	BTS (MPa)	Serpentinization (%)
Very Strong (VS)	Pr-H1	120	8.1	7.7	20 - 30	**Very Strong (VS)**	Px-H1	107	7.0	8.5	20 - 30
	Pr-H2	98	7.6	7.0	25 - 35		Px-H2	137	8.1	9.2	20 - 30
	Pr-H3	115	7.9	8.9	30 - 40		Px-H3	100	5.6	7.3	35 - 45
	Pr-H4	116	8	8.3	25 - 35		Px-H4	135	7.7	9.1	30 - 40
	Pr-H5	104	5.9	7.4	35 - 45		Px-H5	134	7.8	8.7	25 - 35
	Pr-H6	107	5.6	7.2	30 - 40		Px-H6	114	6.3	8.2	35 - 45
	Pr-H7	130	6.9	9.5	25 - 35		Px-H7	98	7.6	7.1	25 - 35
	Pr-H8	130	5.8	9.7	20 - 30		Px-H8	103	5.1	7.2	30 - 40
	Pr-H9	135	7.7	8.6	25 - 35		Px-H9	110	6.9	9.3	25 - 35
	Pr-H10	124	7.2	8.1	30 - 40		Px-H10	100	5.2	6.7	35 - 45
Strong (S)	Pr-M1	69	5.7	5.9	55 - 65	**Strong (S)**	Px-M1	97	5.2	5.7	55 - 65
	Pr-M2	100	5.5	6.9	45 - 55		Px-M2	88	5.7	7.6	35 - 45
	Pr-M3	73	5.1	5.8	35- 45		Px-M3	83	6.2	5.8	50 - 60
	Pr-M4	71	4.8	4.7	50 - 60		Px-M4	66	3.9	6.2	45 - 55
	Pr-M5	79	4.3	5.4	45 - 50		Px-M5	62	4.7	6.9	55 - 65
	Pr-M6	56	3.9	7.9	50 - 60		Px-M6	96	6.3	7.8	40 - 50
	Pr-M7	58	5.9	8.3	45 - 55		Px-M7	87	5.3	5.4	45 - 55
	Pr-M8	49	5.5	5.1	50 - 60		Px-M8	59	5.5	5.7	50 - 60
	Pr-M9	74	6.6	6.7	40 - 50		Px-M9	69	5.9	6.1	35 - 45
	Pr-M10	98	5.9	9.0	35 - 45		Px-M10	67	4.6	6.6	45 - 55
Medium Strong (MS)	Pr-FL1	39	4.4	5.1	55 - 65	**Medium Strong (MS)**	Px-FL1	51	3.8	4.0	70 - 80
	Pr-FL2	49	4.5	3.8	70 - 80		Px-FL2	56	5.3	4.9	70 - 80
	Pr-FL3	52	5.4	3.4	60 - 70		Px-FL3	30	5.8	3.8	60 - 70
	Pr-FL4	58	3.9	6.4	60 - 70		Px-FL4	35	3.7	6.0	55 - 65
	Pr-FL5	48	2.7	3.4	65 - 75		Px-FL5	46	3.4	4.1	65 - 75
	Pr-FL6	31	4.2	3.3	50 - 60		Px-FL6	50	4.1	6.3	55 - 65
	Pr-FL7	27	4.0	3.9	70 - 80		Px-FL7	55	3.3	4.9	60 - 70
	Pr-FL8	30	3.3	4.9	55 - 65		Px-FL8	39	5.6	5.2	65 - 75
	Pr-FL9	43	2.1	5.8	65 - 75		Px-FL9	50	4.2	6.5	65 - 75
	Pr-FL10	35	4.1	3.6	70 - 80		Px-FL10	47	5.2	6.1	60 - 70

The relationship between mechanical parameters with serpentinization

Comparing the results and the percentage of serpentinization shows that in all samples, with an increase in the serpentinization degree, all three types of tested strengths are reduced. These results are compared with each other in Fig. 4. As can be seen, among the strength parameters, the UCS has the closest relationship to the percentage of serpentinization in ultramafic rocks. In the next orders, the BTS and the Is_{50} show a good relationship with the percentage of serpentinization.

As shown in Fig. 4, samples with very high strength (100-250 MPa) exhibit 25-40% serpentinization in the thin sections. In samples with high strength (50-100 MPa), about 40-60% of serpentine is observed and those with a medium strength (25-50 MPa) have 60-75% serpentine. In samples with more than 75% serpentine, the ultramafic minerals are not recognizable and these rocks are considered as serpentinite. It is of note that samples with less than 25% of serpentine were not found in the study area.

Fig. 4 shows serpentinization degrees based on UCS (including MS, S, and VS). This relationship is a plot in the Styles chart (2014) with slight modifications (Fig. 5). According to Table 1, the serpentinization percentage less than 25% is expected to be extra strong and the serpentine percentage of more than 75% is related to the weak and very weak class of UCS.

Fig. 5 presents the relationship between the UCS and the serpentinization degree in the specimens using the Styles *et al.* chart (2014) and classification of UCS (Table 1).

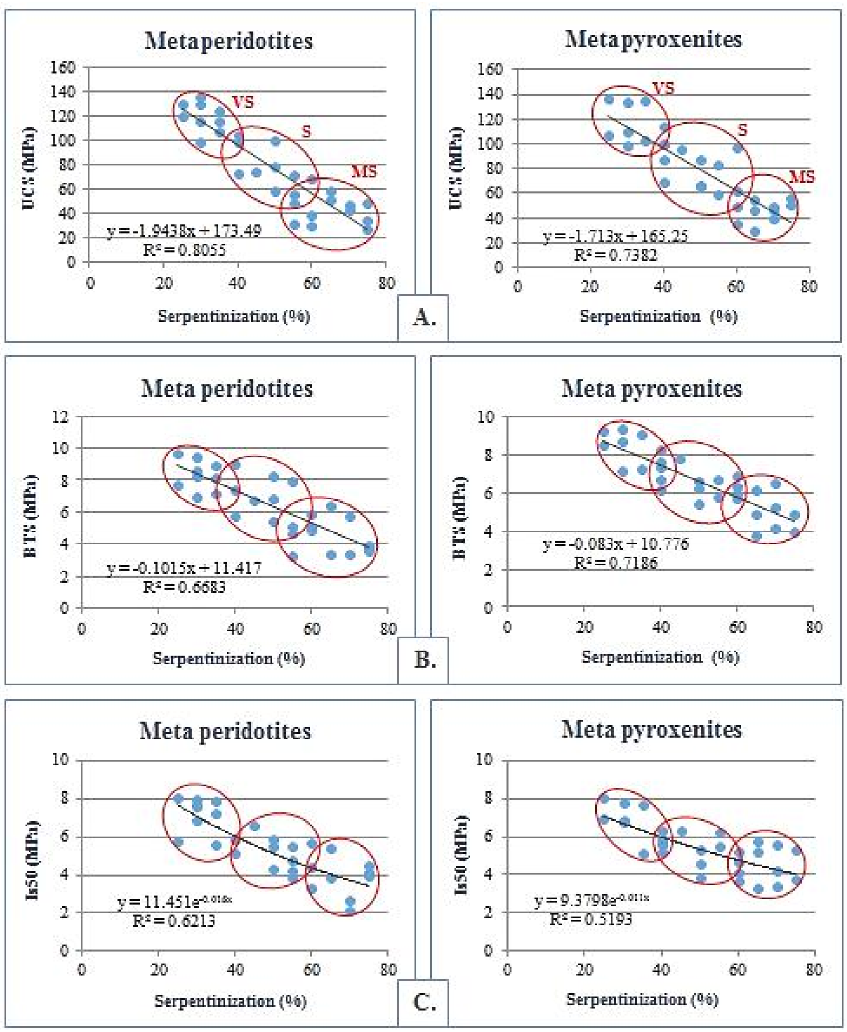

Figure 4. A: Variation of UCS, B: Variation of BTS, C: Variation of Is50 relative to the percentage of serpentinization

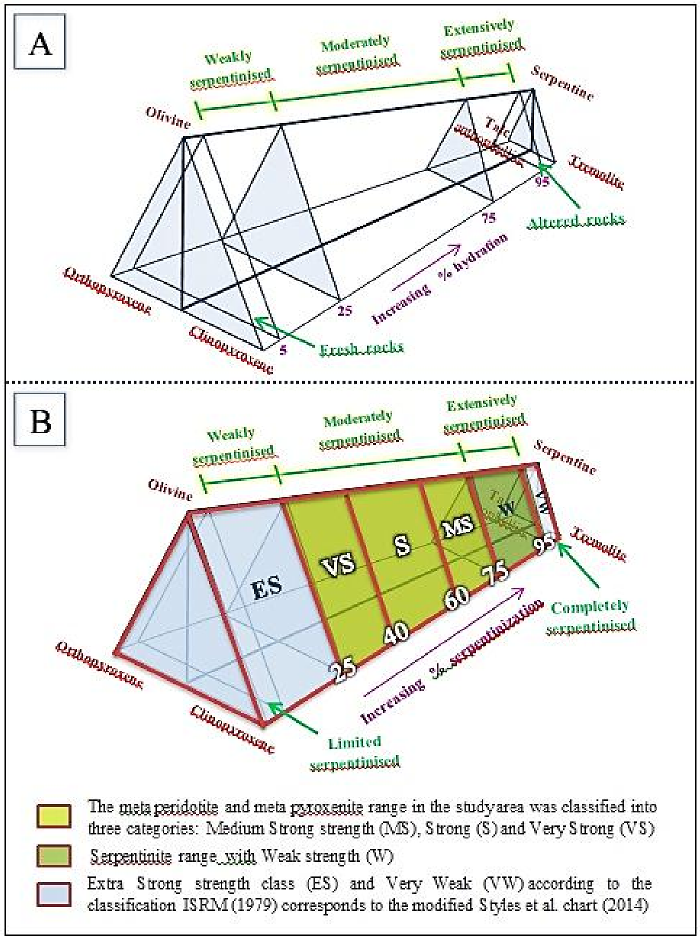

Figure 5. A. Different degrees of serpentinization in ultramafic rocks (Styles *et al*., 2014); B. Modified Styles *et al*. chart (2014) and the relationship between the percentage of serpentinization and UCS based on the three classes of resistance MS, S, and VS in meta-period types and meta-pyroxenites

The relationship between mechanical parameters together

Estimating the strength properties of rocks plays an important role in construction projects such as dams, tunnels, bridges, roads, and underground dams. In all these projects, the objectives such as cost estimation construction time, and safety issues are considered. A precise estimation of the strength properties of rocks is essential for achieving these goals. Therefore, having the necessary information about rock strength such as UCS of the rock is of paramount importance for all kinds of rocks in any project (Armaghani *et al.*, 2015). However, accurate measurement of rocks UCS is quite expensive and time-consuming and has limitations in sample preparation. Considering the importance of the cost and time in engineering projects, many researchers have tried to predict mechanical properties of different rock types using simple methods (Lashkaripour, 2002; Karakus & Tutmez, 2006; Kilic & Teymen, 2008; Rabbani *et al.*, 2012; Aligholi *et al.*, 2017a, 2017b). Some research studies have proposed relationships between the UCS of rocks and characteristic features such as Is_{50}, in order to predict the UCS of the rocks (Yilmaz & Yuksek, 2008; Diamantis *et al.*, 2009; Mishra & Maeda, 2012; Kahraman, 2014; Wong *et al.*, 2017; Zein *et al.*, 2018).

Some other works also have proposed relationships between the UCS of rocks and the BTS in order to predict the UCS of the rocks (Briševac *et al.*, 2015; Momeni *et al.*, 2015; Karaman *et al.*, 2015; Marastoni *et al.*, 2016; Rajabi *et al.*, 2017; Everall & Sanislav, 2018).

In this study, we attempted to provide an appropriate empirical relationship between mechanical parameters. As shown in Fig. 6, the relationship between UCS and BT is different in the two groups of meta-peridotites and meta-pyroxenites. The correlation coefficient in meta-peridotites is approximately 67% while in meta-pyroxenites it is approximately 64% (Fig. 6A).

Fig. 6B shows the relationship between UCS and Is_{50}. The correlation coefficient in this relationship in meta-peridotites is approximately 63% while in meta-pyroxenites it is approximately 57% (Fig. 6B).

Fig. 6C shows the relationship between BTS and Is_{50}. According to this chart, there is a poor correlation between these two parameters such that the coefficient of determination in meta-peridotites and meta-pyroxenites is approximately 30% and 44%, respectively (Fig. 5C).

As a result and according to Fig. 6, among the mechanical parameters, the best relationship in the studied samples is between BTS and UCS.

As shown in Fig. 4, one of the parameters effective on these relationships (Fig. 6) is the serpentinization degree in these rocks. The serpentinization degree in these rocks also is effective on their failure type. Fig. 7A presents examples of UCS failure, Fig. 7B shows examples of the BTS, and Fig. 7C shows examples of the Is50 in three resistance classes before and after the test.

Physical properties

The physical properties of the studied samples such as density, porosity, and water absorption for ultramafic rocks determined based on the standard method of ISRM (1981) are presented in Table 3.

The relationship between physical parameters with serpentinization

Figure 8 shows the relationship between the determined physical properties and the percentage of serpentinization in meta peridotite and meta pyroxenite samples. As shown in Fig. 8 shows the relationship between the determined physical properties and the percentage of serpentinization in meta-peridotite and meta-pyroxenite samples.

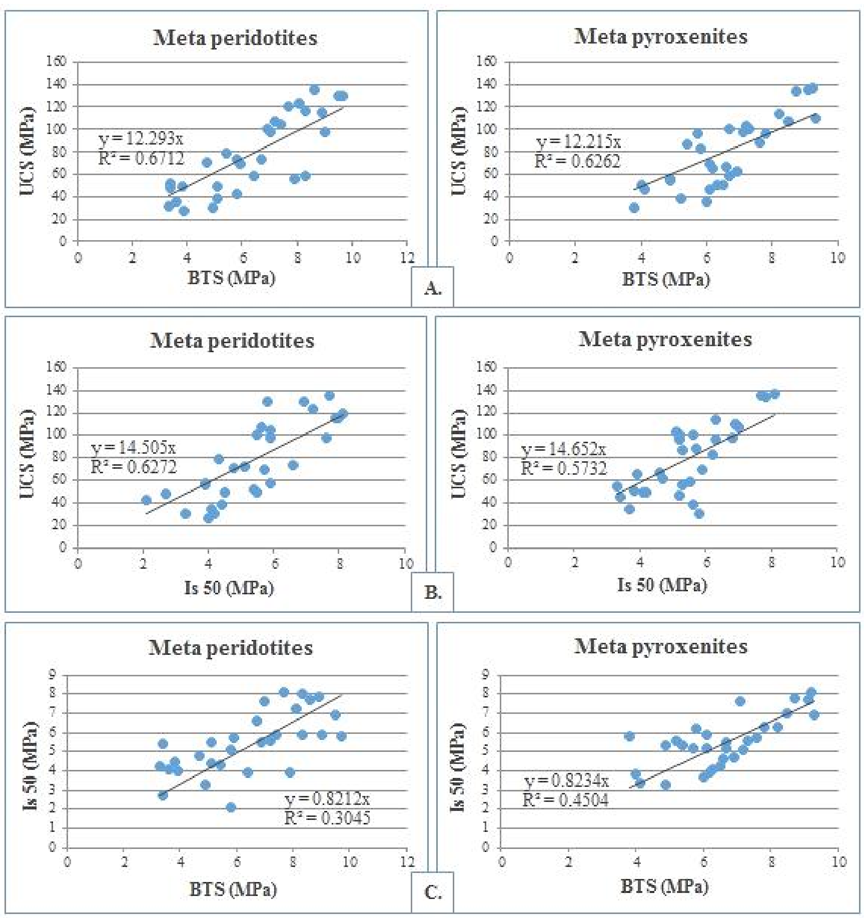

Figure 6. The relationship between A. UCS and BTS, B. UCS and Is_{50}, and C. BTS and Is_{50}

Table 3. Results of physical experiments performed on meta-peridotites and meta pyroxenites

Meta peridotites						**Meta pyroxenites**					
Resistive classification	Sample number	Density (gr/cm^3)	Water absorption (%)	Porosity (%)	Serpentinization (%)	**Resistive classification**	Sample number	Density (gr/cm^3)	Water absorption (%)	Porosity (%)	Serpentinization (%)
Very Strong (VS)	Pr-VS1	3.30	1.6	0.81	20 - 30	**Very Strong (VS)**	Px-VS1	3.22	2.6	0.57	20 - 30
	Pr-VS2	3.18	2.9	0.68	25 - 35		Px-VS2	3.31	1.4	0.52	20 - 30
	Pr-VS3	3.05	1.9	0.90	30 - 40		Px-VS3	3.00	2.5	0.86	35 - 45
	Pr-VS4	3.28	1.5	0.41	25 - 35		Px-VS4	3.17	1.5	0.62	30 - 40
	Pr-VS5	2.99	3.2	0.73	35 - 45		Px-VS5	3.24	2.2	0.52	25 - 35
	Pr-VS6	3.21	1.7	0.45	30 - 40		Px-VS6	3.27	1.9	0.74	35 - 45
	Pr-VS7	3.32	2.1	0.51	25 - 35		Px-VS7	3.31	1.3	0.51	25 - 35
	Pr-VS8	3.11	2.7	0.57	20 - 30		Px-VS8	3.29	1.7	0.66	30 - 40
	Pr-VS9	3.08	1.5	0.50	25 - 35		Px-VS9	3.11	2.8	0.70	25 - 35
	Pr-VS10	3.25	2.3	1.03	30 - 40		Px-VS10	3.25	2.4	0.64	35 - 45
Strong (S)	Pr-S1	2.89	3.9	0.95	55 - 65	**Strong (S)**	Px-S1	3.07	2.2	1.21	55 - 65
	Pr-S2	2.60	3.4	1.26	45 - 55		Px-S2	3.21	1.9	0.69	35 - 45
	Pr-S3	3.12	1.9	0.74	35- 45		Px-S3	2.98	3.2	0.85	50 - 60
	Pr-S4	2.95	2.0	0.85	50 - 60		Px-S4	2.64	3.9	1.82	45 - 55
	Pr-S5	2.56	2.8	0.91	45 - 50		Px-S5	2.85	3.5	0.72	55 - 65
	Pr-S6	2.25	4.2	1.99	50 - 60		Px-S6	3.01	1.9	0.67	40 - 50
	Pr-S7	2.81	2.3	0.62	45 - 55		Px-S7	2.84	1.8	0.53	45 - 55
	Pr-S8	2.66	2.8	1.80	50 - 60		Px-S8	2.87	3.2	1.02	50 - 60
	Pr-S9	3.22	1.5	0.66	40 - 50		Px-S9	2.95	2.1	1.07	35 - 45
	Pr-S10	2.79	3.1	1.34	35 - 45		Px-S10	2.82	2.3	0.87	45 - 55
Medium Strong (MS)	Pr-MS1	2.64	7.1	2.97	55 - 65	**Medium Strong (MS)**	Px-MS1	2.85	2.6	1.27	70 - 80
	Pr-MS2	2.59	3.1	0.90	70 - 80		Px-MS2	2.71	2.8	0.71	70 - 80
	Pr-MS3	2.54	3.4	1.57	60 - 70		Px-MS3	2.82	2.5	0.73	60 - 70
	Pr-MS4	2.42	5.5	2.14	60 – 70		Px-MS4	2.69	3.5	1.32	55 – 65
	Pr-MS5	2.39	4.5	1.84	65 – 75		Px-MS5	2.88	2.9	0.92	65 – 75
	Pr-MS6	2.34	3.7	1.53	50 – 60		Px-MS6	2.73	4.5	1.06	55 – 65
	Pr-MS7	2.60	4.4	3.39	70 – 80		Px-MS7	2.48	3.7	1.97	60 – 70
	Pr-MS8	2.46	3.2	1.85	55 – 65		Px-MS8	2.56	4.2	2.16	65 – 75
	Pr-MS9	2.52	6.3	2.13	65 – 75		Px-MS9	2.77	3.0	1.02	65 – 75
	Pr-MS10	2.80	3.7	1.17	70 – 80		Px-MS10	2.84	2.9	0.98	60 – 70

Figure 7. To be continued

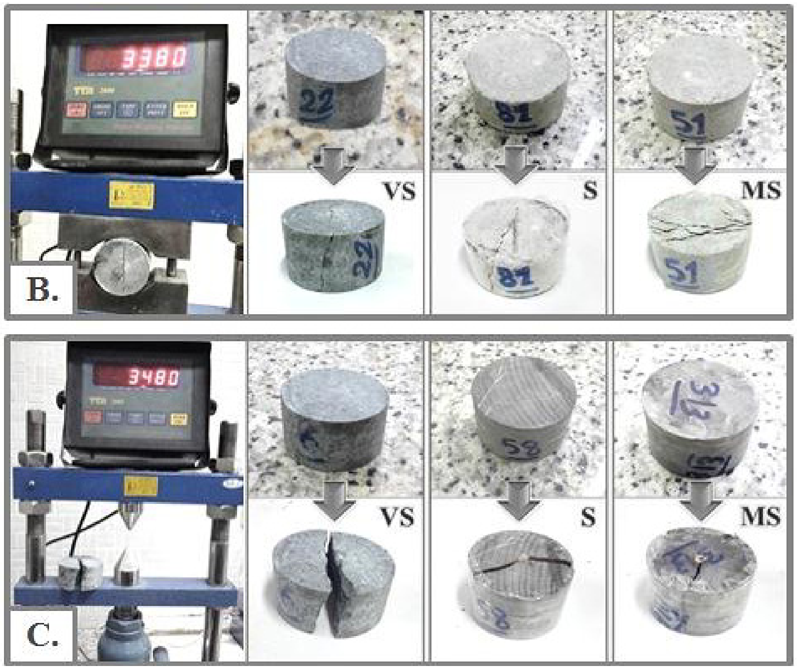

Figure 7. A: Examples of UCS in three resistance classes before and after the test, B: Examples of (BTS) in three resistance classes before and after the test, and C: Examples of (Is_{50}) in three resistance classes before and after the test and their failure types

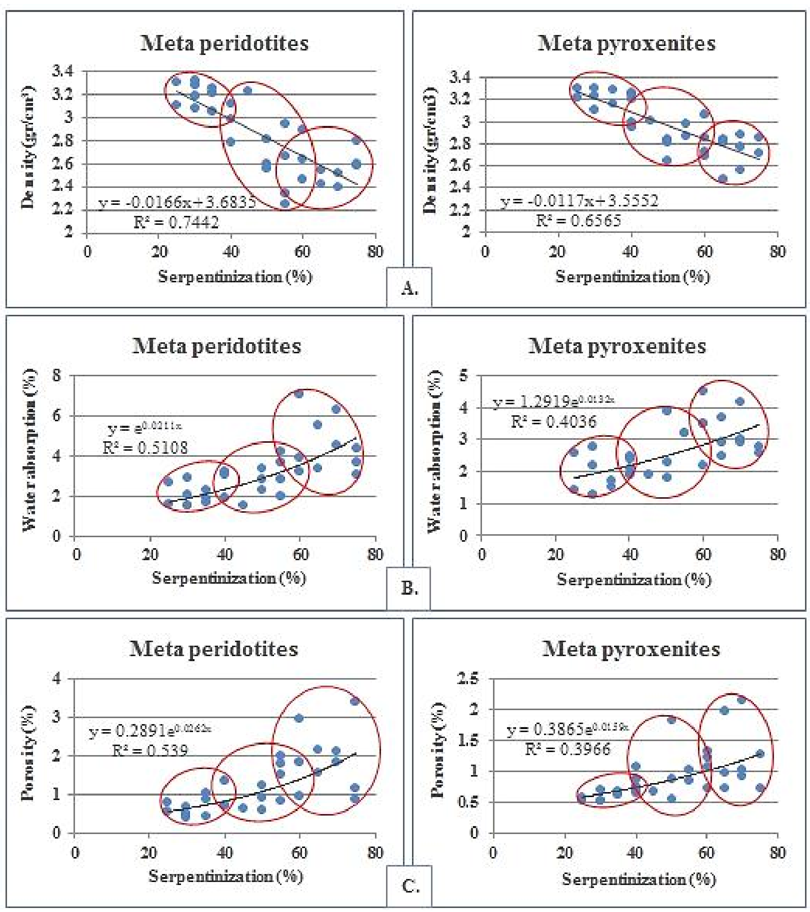

Figure 8. Variations of A. density (gr/cm^3), B: water absorption (%), and C: porosity (%) relative to the serpentinization percentage

As shown in Fig. 8A, the relationship between the density with the serpentinization percentage degree is inverse such that with increasing the serpentinization degree, the density is decreasing. In comparison, water absorption and porosity percentage show a direct exponential relation with serpentinization degree (Figs. 8B and 8C) and both parameters increase with increasing serpentinization degree. As can be seen, the degree of serpentinization affects all three physical parameters so that this relationship is more coherent in higher values of density and low amounts of water absorption and porosity.

The relationship between physical parameters together

Fig. 9 shows the relationship between physical parameters. As shown in Fig. 9A, the relationship between water absorption and porosity has a direct exponential form. As can be seen, the correlation coefficient in meta-peridotites is approximately 66% while in meta-pyroxenites it is approximately 53% (Fig. 9A).

Water absorption and density have an inverse exponential relation with each other (Fig. 9B). In this relationship, the correlation coefficient in meta-peridotites is approximately 59% and in meta-pyroxenites, it is about 60%.

Also, the relationship between density and porosity is in direct exponential form. In this relationship, the correlation coefficient in meta-peridotites is approximately 63% and in meta-pyroxenites is approximately 60% (Fig. 9C).

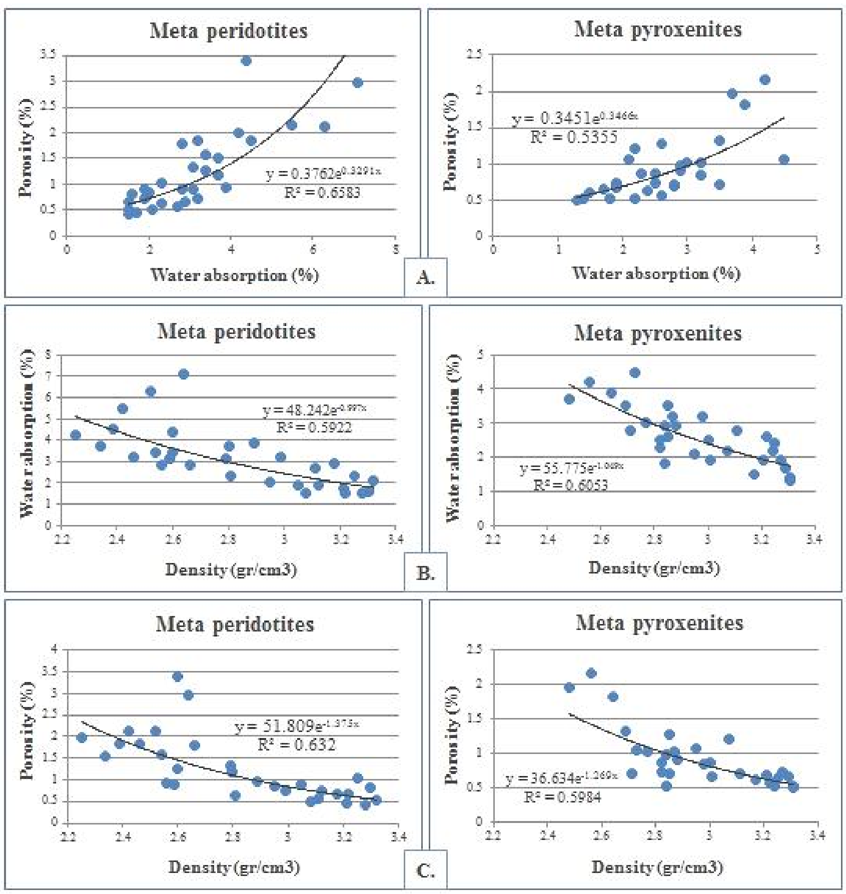

Figure 9. The relationship between: A. porosity (%) and water absorption (%), B: water absorption (%) and density (gr/cm^3), C: porosity (%) and density (gr/cm^3)

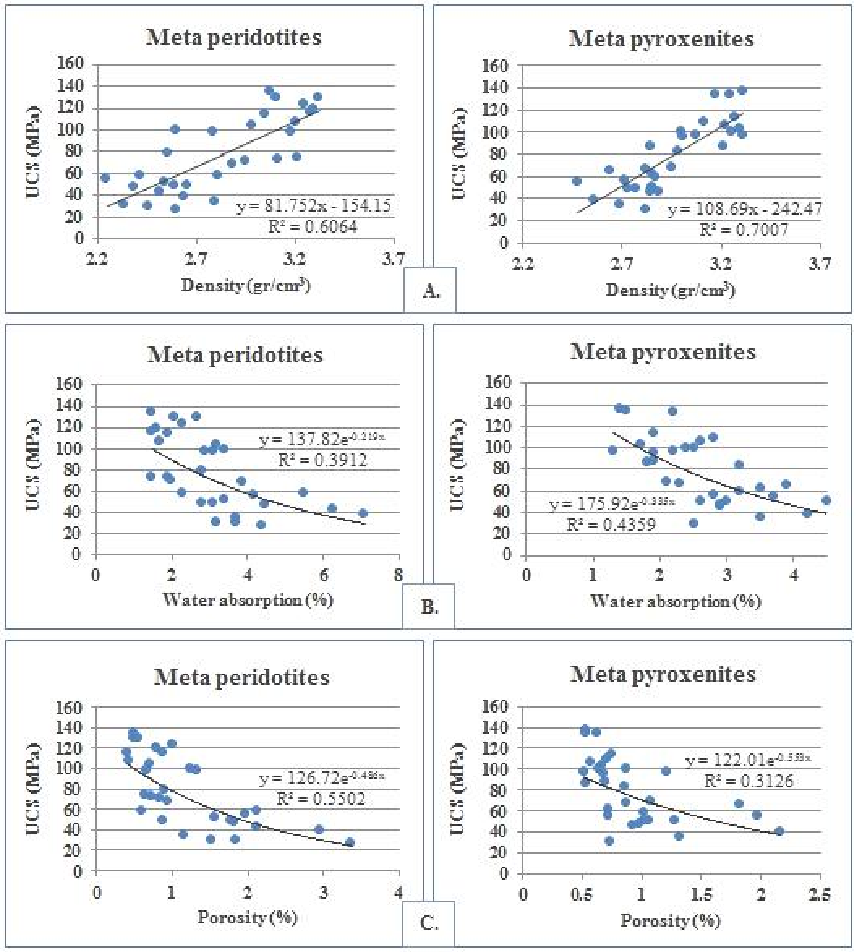

Figure 10. The relationship between A: UCS (MPa) and density (gr/cm^3), B: UCS (MPa) and water absorption (%), C: UCS (MPa) and porosity (%)

The relationship between physical parameters with UCS

Considering that among the studied mechanical parameters the UCS is of higher significance, the relationship between physical parameters and UCS is investigated in Fig. 10.

Comparing the relationship between UCS and physical parameters shows a more regular relationship between UCS and density in both groups of rocks with a correlation coefficient of more than 60% (Fig. 10).

The results show that the percentage of serpentinization in ultramafic rocks greatly affects the parameters and thus it should be considered in evaluating the relationship between these properties. Regarding the role of the serpentinization degree in this relationship, it was attempted to develop another method to demonstrate the relationship between geotechnical parameters and the degree of serpentinization. Based on the obtained test results, Fig. 11 presents a diagram for predicting the UCS from the BTS and density regarding the serpentinization degree.

Comparison of the UCS obtained in the laboratory and the UCS obtained from Fig. 11 for all samples shows that because of considering the serpentinization degree, this graph is more accurate than the equations for predicting UCS of ultramafic rocks. Since the serpentinization degree shows a linear and inverse relationship with density, in cases where microscopic studies are not feasible, the density of the samples can be used instead of serpentinization degree and UCS can be approximated using the BTS.

The comparison between laboratory results and field observations shows that the field behavior of rock masses also can be used to predict a UCS range. However, because the serpentines of the region have formed during the Paleozoic due to metamorphism and are not a product of weathering, weathering signs cannot be used to identify them. Table 4 compares the samples and different degrees of serpentinization with the field behavior of rock masses.

According to the field behavior of rock masses, the range of UCS and serpentinization degree can be predicted for the case when a range of UCS or serpentinization degree is required. Figs. 12A to 12D show an example of rock masses in the study area that its group has been identified based on the field identification in Table 4. The laser meter has been used to determine the height of the rock mass. Figs. 12A, 12B, 12C, and 12D present the resistance classes (i.e., VS, S, MS, and W), (S, MS, W), (MS, W), (W), respectively.

Table 4. Field behavior of ultramafic rock masses in the studied area

Rock group	Classification by serpentine value	Serpentinization percentage	Group sign	Field Detection	uniaxial compressive strength (UCS)
meta peridotites and meta pyroxenites	Moderate Serpentinitis	25 – 40	**VS**	The rock mass has a crack	100 – 250 MPa
		40 - 60	**S**	The rock mass has a fracture and the edges of the fractures are sharp	50 – 100 MPa
		60 – 75	**MS**	The stone is crushed and the edges of the fractures are soft	25 – 50 MPa
Serpentinites	Extensively serpentinised	75 – 95	**W**	The rock mass is completely touching the soap	5 – 25 MPa

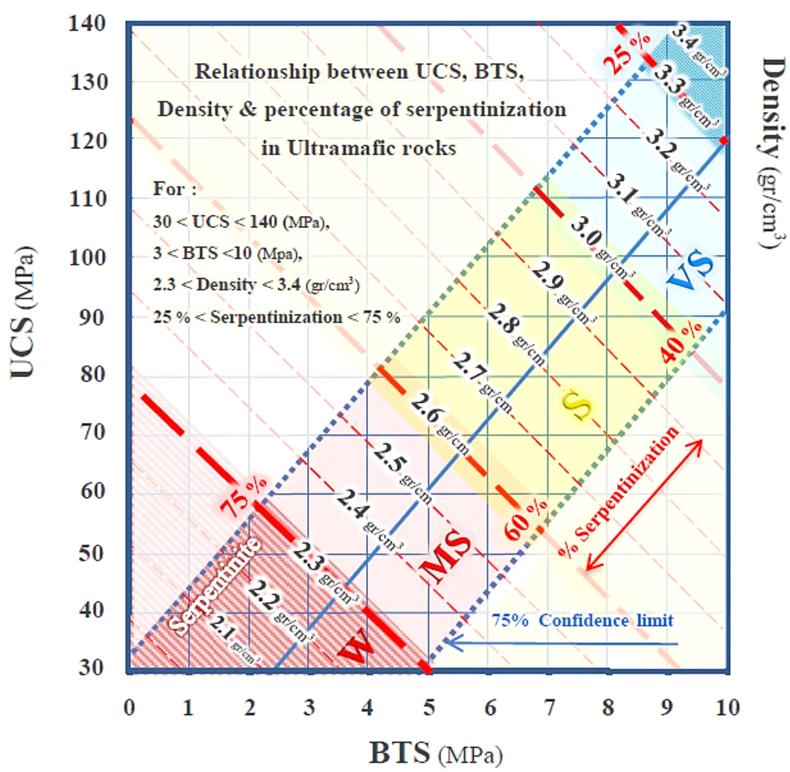

Figure 11. The relationship between UCS, BTS, and density with respect to the percentage of serpentinization in ultramafic rocks

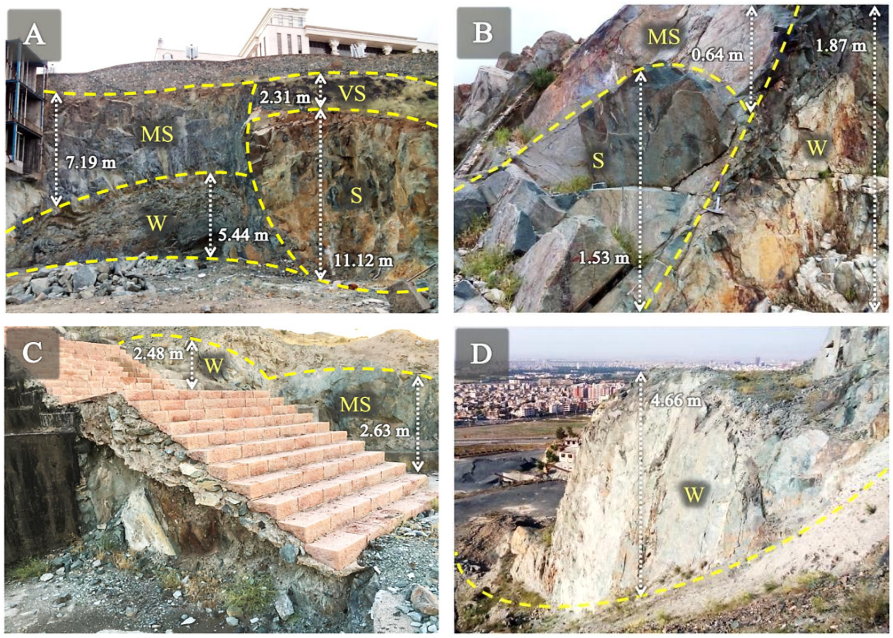

Figure 12. Examples of field behavior of rock mass in the studied area. A: resistance classes VS, S, MS, and W; B: resistance classes S, MS, and W; C: Resistance classes MS, W; and D: Resistance class W.

Conclusions

Serpentinization of ultramafic rocks in the southwest of Mashhad is due to subduction of Palaeo-Tethys and regional metamorphism of ophiolites. Serpentines formed at that time until the present have been influenced by active tectonics. Therefore, trusts have different degrees of serpentinization in the ultramafic rocks of the region. The present research demonstrates the influence of serpentinization degree on the geotechnical properties of ultramafic rocks such that with increasing serpentinization, UCS, the BTS, Is50, and density parameters are reduced while the water absorption percentage and porosity percentage increase. Considering a better relationship between the serpentinization degrees and the UCS, the BTS, and density, a graph was proposed to predict UCS through BTS and density, which also incorporates the serpentinization degree of the rocks. Considering the percentage of serpentinization, the UCS obtained from this graph provides a higher accuracy compared to that obtained from the formulas available. Also, field observations based on the signs presented can predict a range of UCS and a range of serpentinization degrees in ultramafic rocks. According to the results of this study, in the ultramafic rocks of the study area, it is recommended considering the serpentinization percentage such that to more accurately predict the resistance parameters.

References

Abdelaziz, R., Abdel-Rahman, Y., Wilhelm, S., 2018. Landsat-8 data for chromite prospecting in the Logar Massif, Afghanistan. Heliyon, 4: 1–18.

Aligholi, S., Lashkaripour, GR., Ghafoori, M., 2017a. Strength/Brittleness classification of igneous intact rocks based on basic physical and dynamic properties. Rock Mechanics and Rock Engineering, 50: 45–65.

Aligholi, S., Lashkaripour, GR., Ghafoori, M., TrighAzali, S., 2017b. Evaluating the relationships between NTNU/SINTEF drillability indices with index properties and petrographic data of hard igneous rocks. Rock Mechanics and Rock Engineering, 50: 2929–2953.

Arel, E., Tuğrul, A., 2001. Weathering and its relation to geomechanical properties of Çavuşbaşı granitic rocks in northwestern Turkey. Bulletin Engineering Geology Environ, 60: 123–133.

Armaghani, D.J., Tonnizam, E., Hajihassani, M., Yagiz, S., Motaghedi, H., 2015. Application of several non-linear prediction tools for estimating uniaxial compressive strength of granitic rocks and comparison of their performances. Engineering with Computers, 32: 189–206.

Bieniawski, Z.T., 1974. Estimating the strength of rock materials. Journal of the South African Institute of Mining and

Metallurgy, 74: 312–320.
Boulin, J., 1988. Hercynian and Eocimmerian events in Afghanistan and adjoining regions. Tectonophysics, 148: 253-278.
Brisevac, Z., Kujundzic, T., Cajic, S., 2015. Current Cognition of Rock Tensile Strength Testing By Brazilian Test. The Mining-Geology-Petroleum Engineering Bulletin, 30: 101–114.
Ceryan, S., Tudes, S., Ceryan, N., 2008. Influence of weathering on the engineering properties of Harsit granitic rocks (NE Turkey). Bulletin Engineering Geology Environ, 67: 97–104.
Christensen, N.I., 1966. Shear-wave vetocities in metamorphic rocks at pressures to 10 kbar. Journal of Geophysical Research, 71:3549–3556.
Christensen,N.I., 2004. Serpentinites, peridotites and seismology. International Geology Review, 46: 795–816.
Courtier, A., Hart, D., Christensen, N.I., 2004. Seismic properties of leg 195 serpentinites and their geophysical implications. Proceedings of the Ocean Drilling Program Scientific Results, 195: 1–12.
Dobretsov, N.L., 1974. Glaucophane metamorphism and three types of ophiolite complexes. Doklady Akademii Nauk SSSR, 216 (6): 1383–1386.
Dobretsov, N.L., Moldavantsev, Yu.E., Kazak, A.P., Ponomareva, L.G., Savel'eva, G.N., Savel'ev, A.A., 1977. Petrology and Metamorphism of Ancient Ophiolites (by the Example of the Arctic Urals and West Sayan) [in Russian]. Nauka, Novosibirsk.
Dobretsov, N.L., 1980. Introduction to Global Petrology [in Russian]. Nauka, Novosibirsk.
Dobretsov, N.L., 1985. Riphean–Lower Paleozoic Ophiolites of Northern Eurasia [in Russian]. Nauka, Novosibirsk.
Dobretsov, N.L., Konnikov, E.G., Sklyarov, E.V., Medvedev, V.N., 1986. Marianite-boninite series and evolution of ophiolite magmatism of East Sayan. Soviet Geology and Geophysics, 27 (12): 29–35.
Dobretsov, N.L., Watanabe, T., Natal'in, B., Miyashita, S., 1994. Comparison of ophiolites and blueschists of Sakhalin and Hokkaido. Ofioliti, 19: 157–176.
Diamantis, K., Gartzos, E., Migiros, G., 2009. Study on uniaxial compressive strength, point load strength index, dynamic and physical properties of serpentinites from Central Greece: test results and empirical relations. Engineering Geology, 108: 199-207.
Diamantis, K., 2010. Engineering geological properties of the ultrabasic rocks in Othrys and Kallidromo mountains (central Greece). Phd Thesis, Athens, 386 pp.
Escartin, J., Hirth, G., Evans, B., 2001. Strength of slightly serpentinized peridotites:mplications for the tectonics of oceanic lithosphere. Geological Society of America, 29(11): 1023–1026.
Everall, T., Sanislav, J., 2018. The Influence of Pre-Existing Deformation and Alteration Textures on Rock Strength, Failure Modes and Shear Strength Parameters. Geosciences, 8: 124-138.
Faust, G. T., Fahey, J. J., 1964. The Serpentine-Group Minerals. Correlation of the physical and chemical properties in terms of crystal chemistry and the application of geo chemical data to thepetrogenesis of serpentine and ultrabasic rocks. United states government printing office, Washington, 384 pp.
Hynes, A., 1975. Comment on "The Troodos ophiolitic complex was probably formed in an island arc", by A. Miyashiro. Earth and Planetary Science Letters, 25: 2l3–216.
ISRM, 1978. Suggested methods for determining tensile strength of rock materials. International Journal of Rock Mechanics and Mining Sciences, 15: 99–103.
ISRM, 1979. Suggested methods for determining the uniaxial compressive strength and deformability of rock materials, International Journal of Rock Mechanics and Mining. Sciences and Geomechanics Abstracts, 16: 135-140.
ISRM, 1981. In: Brown, E.T. (Ed), ISRM Suggested Methods: Rock Characterization, Testing and Monitoring. Pergamon Press, London, 211 p.
ISRM, 1985. Suggested methods for determining point load strength. , International Journal of Rock Mechanics and Mining. Sciences and Geomechanics Abstracts, 22: 51–60.
ISRM, 2007. In: Ulusay R, Hudson JA (eds) The complete ISRM suggested methods for rock characterization, testing and monitoring: 1974–2006. Suggested methods prepared by the commission on testing methods, International Society for Rock Mechanics, compilation arranged by the ISRM Turkish National Group. Ankara, Turkey, p 628.
Kahraman, S., 2014. The determination of uniaxial compressive strength from point load strength for pyroclastic rocks. Engineering Geology, 170: 33-42.
Karakus, M., Tutmez, B., 2006. Fuzzy and multiple regression modelling for evaluation of intact rock strength based on point load, Schmidt hammer and sonic velocity. Rock Mechanics and Rock Engineering, 39: 45–57.
Karaman, K., Cihangir, F., Ercikdi, B., Kesimal, A., Demirel, S., 2015. Utilization of the Brazilian test for estimating the uniaxial compressive strength and shear strength parameters. The Journal of the southern African institute of Mining and Metallurgy, 115: 185-192.
Khanchuk, A. I., Vysotskiy, S. V., 2015. Different-depth gabbro–ultrabasite associations in the Sikhote-Alin ophiolites (Russian Far East). Russian Geology and Geophysics, 57: 141–154.

Kiliç, R., Koçbay, A., Sel, T., 1998. The geomechanical properties and alteration degree of serpentinite in the Ankara Ophiolitic Melange, Turkey. In: 8th International IAEG Congress, Proceedings, Vancouver, 1: 243–251.
Kilic, A., Teymen, A., 2008. Determination of mechanical properties of rocks using simple methods. Bulletin Engineering Geology Environ, 67: 237–244.
Koumantakis, J., 1982. Comportement des peridotites et serpentinites de la Grece en travaux public. Leur propretes physiques et mechaniques, Bulletin of the International association of engineering geology, 25: 53–60.
Lashkaripour, GR., 2002. Predicting mechanical properties of mudrock from index parameters. Bulletin of Engineering Geology and the Environment, 61: 73–77.
Marastoni, D., Pela, L., Benedetti, A., Roca, P., 2016. Combining Brazilian tests on masonry cores and double punch tests for the mechanical characterization of historical mortars. Construction and Building materials, 112: 112–127.
Marinos, P., Hoek, E., Marinos, V., 2006. Variability of the engineering properties of rock masses quantified by the geological strength index: the case of ophiolites with special emphasis on tunneling. Bulletin of Engineering Geology and the Environment, 65: 129–142.
Markov, M.S., Nekrasov, G.E., Khotin, M.Yu., Sharas'kin, A.Ya., 1977. Petrochemical peculiarities of ophiolites and some problems of their genesis. Geotektonika, 6: 15–31.
Mishra, DA., Basu, A., 2012. Use of the block punch test to predict the compressive and tensile strengths of rocks. International Journal of Rock Mechanics and Mining Sciences, 51: 119-127.
Miyashiro, A., 1975. Classification, characteristics and origin of ophiolites, Journal of Geology, 83: 249–291.
Coleman, R.G., 1977. Ophiolites: Ancient Oceanic Lithosphere? Springer-Verlag, Berlin, Heidelberg, New York.
Momeni, A.A., Khanlari, GR., Heidari, M., Sepahi, A. A., Bazvand, E., 2015. New engineering geological weathering classifications for granitoid rocks. Engineering Geology, 185: 43-51.
Moores, E.M., 1975. Discussion of "Origin of Troodos and other ophiolites: A reply to Hynes", by Akiho Miyashiro. Earth and Planetary Science Letters, 25: 223–226.
Ozsoy, E.A., Yilmaz, G., Arman, H., 2010. Physical, mechanical and mineralogical properties of ophiolitic rocks at the Yakakayi dam site, Eskisehir, Turkey. Scientific Research and Essays, 5(17): 2579–2587.
Paventi, M., Scoble, M., Stead, D., 1996. Characteristics of a complex serpentinised ultramafic rock mass at the Birchtree Mine. Manitoba. In: Mitri, H. Aubertin (Ed.), North American Rock Mechanics Symposium. Rotterdam, 1: 339–346.
Přikryl, R., 2006. Assessment of rock geomechanical quality by quantitative rock fabric coefficients: Limitations and possible source of misinerpretations. Engineering Geology, 87: 149–162.
Pola, A., Crosta, G., Fusi, N., Barberini, V., Norini, G., 2012. Influence of alteration on physical properties of volcanic rocks. Tectonophysics, 566: 67–86.
Pola, A., Crosta, G.B., Fusi, N., Castellanza, R., 2014. General characterization of the mechanical behaviour of different volcanic rocks with respect to alteration. Engineering Geology, 169: 1–13.
Promyslova, M. Yu., Demina, L. I., Bychkov, A. Yu., Gushchin, A. I., 2016. Ophiolitic Association of Cape Fiolent Area, Southwestern Crimea. Geotectonics, 50: 21-34.
Rabbani, E., Sharif, F., KoolivandSalooki, M., Moradzadeh, A., 2012. Application of neural network technique for prediction of uniaxial compressive strength using reservoir formation properties. International Journal of Rock Mechanics and Mining Sciences, 56: 100–111.
Rajabi, A., Omidi Moaf, F., 2017. Simple empirical formula to estimate the main geomechanical parameters of preplaced aggregate concrete and conventional concrete. Construction and Building Materials, 146: 485–492.
Rao, M.V.M.S., Ramana, Y.V., 1974. Dilatant Behaviour of Ultramafic Rocks during Fracture. International Journal of Rock Mechanics and Mining Sciences, Geomechanics abstract, Pergamon Press, 227(1-4): 193–203.
Rigopoulos, I., 2009. Correlation between petrographic and physico-mechanical properties of the Pindos and Vourinos ophiolitic rocks and assessment of their suitability as aggregates in construction-industrial uses. PhD thesis, University of Patras.
Rigopoulos, I., Tsikouras, B., Pomonis, P., Hatzipanagiotou, K., 2010. The influence of alteration on the engineering properties of dolerites: The examples from the Pindos and Vourinos ophiolites (northern Greece). International Journal of Rock Mechanics and Mining Sciences, 47: 69–80.
Rigopoulos, I., Tsikouras, B., Pomonis, P., Hatzipanagiotou, K., 2012. The impact of petrographic characteristics on the engineering properties of ultrabasic rocks from central and northern Greece, Quarterly Journal of Engineering Geology and Hydrogeology, 45: 423–433.
Rigopoulos, I., Tsikouras, B., Pomonis, P., Hatzipanagiotou, K., 2013. Determination of the interrelations between the engineering parameters of construction aggregates from ophiolite complexes of Greece using factor analysis. Construction and Building Materials, 49: 747–757.
Shcheglov, A.D., Bur'yanova, I.Z., Vasil'kovskii, N.P., Govorov, I.N., Shcheka, S.A. (Eds.), 1984. Volcanic Belts in Eastern Asia [in Russian]. Nauka, Moscow.
Siratovich, P.A., Heap, M.J., Villenueve, M.C., Cole, J.W., Reuschlé, T., 2014. Physical property relationships of the

Rotokawa Andesite, a significant geothermal reservoir rock in the Taupo Volcanic Zone, New Zealand, Geothermal energy, 2(1): 10–31.

Sonmez, H., Tuncay, E., Gokceoglu, C., 2004. Models to predict the uniaxial compressive strength and the modulus of elasticity for Ankara agglomerate. International Journal of Rock Mechanics and Mining Sciences, 41 (5): 717–729.

Sonmez, H., Gokceoglu, C., Medley, E.W., Tuncay, E., Nefeslioglu, H.A., 2006. Estimating the uniaxial compressive strength of a volcanic bimrock. International Journal of Rock Mechanics and Mining Sciences, 43(4): 554–561.

Stampfli, G.M., 1996. The intra-alpine terrain: a Paleo-Tethyan remnant in the alpine variscides. Eclogae Geologicae Helvetiae, 89: 13–42.

Styles, M.T., Sanna, A., Lacinska, A.M., Naden, J. and Maroto-Valer, M., 2014. The variation in composition of ultramafic rocks and the effect on their suitability for carbon dioxide sequestration by mineralization following acid leaching. Modeling and Analysis, 4(1): 1-12.

Ündül, Ö., Tuğrul, A., 2012. The influence of weathering on the engineering properties of dunites. Rock Mechanics and Rock Engineering, 45: 225-239.

Vysotskiy, S.V., 1989. Ophiolite Associations of the Pacific Island-Arc Systems [in Russian]. Izd. DVO AN SSSR, Vladivostok.

Vysotskiy, S.V., 1996. Ophiolite and Boninite–Ophiolite Associations of the West Pacific Island-Arc Systems. ScD Thesis. MGU, Moscow.

Wong, R., Chau, KT., Yin, J., Lai, D., Zhao, G., 2017. Uniaxial compressive strength and point load index of volcanic irregular lumps. International journal of rock mechanics & mining sciences, 93: 307-315.

Wyering, L.D., Villeneuve, M.C., Wallis, I.C., Siratovich, P.A., Kennedy, B.M., Gravley, D.M., Cant, J.L., 2014. Mechanical and physical properties of hydrothermally altered rocks, Taupo Volcanic Zone, New Zealand. Journal of Volcanology and Geothermal Research, 288: 76-93.

Yilmaz, I., Yuksek, A.G., 2008. An example of artificial neural network (ANN) application for indirect. Rock Mechanics and Rock Engineering, 41: 781-795.

Zanchi, A., Zanchetta, S., Berra, F., Mattei, M., Garzanti, E., Molyneux, S., Nawab, A. and Sabouri, J., 2009. The Eo-Cimmerian (Late? Triassic) orogeny in north Iran. In: Brunet, M.-F.,Wilmsen, M., Granath, J.W. (Eds.), South Caspian to Central Iran Basins. Geological Society of London Special Publication, 312: 31-55.

Zein, A., Sandal, M., 2018. Estimation of the strength of Nubian sandstone formation from point load test index and other simple parameters MATEC Web of Conferences 149, 02024, 6 pages, Doi.org/10.105/matecconf.